Addressable adsorption of lipid vesicles and subsequent protein interaction studies

Goran Klenkar, Björn Brian,[a] and Thomas Ederth
Division of Molecular Physics, Department of Physics, Chemistry and Biology, Linköping University, SE-58183 Linköping, Sweden

Gudrun Stengel and Fredrik Höök
Division of Biological Physics, Department of Applied Physics, Chalmers University of Technology, SE-41296 Göteborg, Sweden

Jacob Piehler
Institute of Biochemistry, Johann Wolfgang Goethe-University, Max-von-Laue-Str. 9, 60438 Frankfurt, Germany

Bo Liedberg[b]
Division of Molecular Physics, Department of Physics, Chemistry and Biology, Linköping University, SE-58183 Linköping, Sweden

(Received 13 March 2008; accepted 15 April 2008; published 6 June 2008)

We demonstrate a convenient chip platform for the addressable immobilization of protein-loaded vesicles on a microarray for parallelized, high-throughput analysis of lipid-protein systems. Self-sorting of the vesicles on the microarray was achieved through DNA bar coding of the vesicles and their hybridization to complementary strands, which are preimmobilized in defined array positions on the chip. Imaging surface plasmon resonance in ellipsometric mode was used to monitor vesicle immobilization, protein tethering, protein-protein interactions, and chip regeneration. The immobilization strategy proved highly specific and stable and presents a mild method for the anchoring of vesicles to predefined areas of a surface, while unspecific adsorption to both noncomplementary regions and background areas is nonexistent or, alternatively, undetectable. Furthermore, histidine-tagged receptors have been stably and functionally immobilized via *bis*-nitrilotriacetic acid chelators already present in the vesicle membranes. It was discovered though that online loading of proteins to immobilized vesicles leads to cross contamination of previously loaded vesicles and that it was necessary to load the vesicles offline in order to obtain pure protein populations on the vesicles. We have used this cross-binding effect to our benefit by coimmobilizing two receptor subunits in different ratios on the vesicle surface and successfully demonstrated ternary complex formation with their ligand. This approach is suitable for mechanistic studies of complex multicomponent analyses involving membrane-bound systems. [DOI: 10.1116/1.2921867]

I. INTRODUCTION

Over the past ~15 years, a lot of effort has been put into research and development of miniaturized microarray assays.[1–6] The fundamental features of the microarray concept is high throughput through parallel monitoring of many interactions on a high-density surface, onto which many biomolecules have already been immobilized. By following in the footsteps of the successful DNA microarrays,[1–3] protein microarrays have been developed.[4–6] Protein microarrays are generally believed to be a potentially highly valuable tool as proteins are the fundamental regulatory entities in an organism[7] and, consequently, are the main target of pharmaceutical drugs.[8] Furthermore, the elucidation of proteome function including protein interactomes is considered to be the key challenge of postgenomic life science research.

About 30% of the open reading frames of human genome encode for integral or associated membrane proteins. Moreover, this important part of the proteome accounts for more than 50% of pharmaceutical drug targets.[8] The functional properties of membrane proteins highly depend on the native membrane environment. For this reason, solid-supported lipid membranes and vesicles have been developed as model systems that mimick the cellular membranes.[9] The microarray concept was applied in this field for the study of G protein-coupled receptors (GPCRs), which was successfully reported on micropatterned surfaces with lipid membranes.[10,11] In the work of Fang *et al.*,[11] a microarray of membrane-bound proteins was demonstrated by the printing of vesicular solutions of phospholipids containing GPCRs. An alternative vesicle immobilization procedure was developed, where the high selectivity and sequence variability of DNA were used to mediate the binding of vesicles to predefined regions of a surface.[12–14] Single-stranded DNA (ssDNA) sequences are preimmobilized in positions of the array over which vesicles tagged with complementary single-

[a]Present address: Department of Applied Physics, Chalmers University of Technology, Origov. 6B, SE-41296 Göteborg, Sweden.
[b]Author to whom correspondence should be addressed; electronic mail: bol@ifm.liu.se

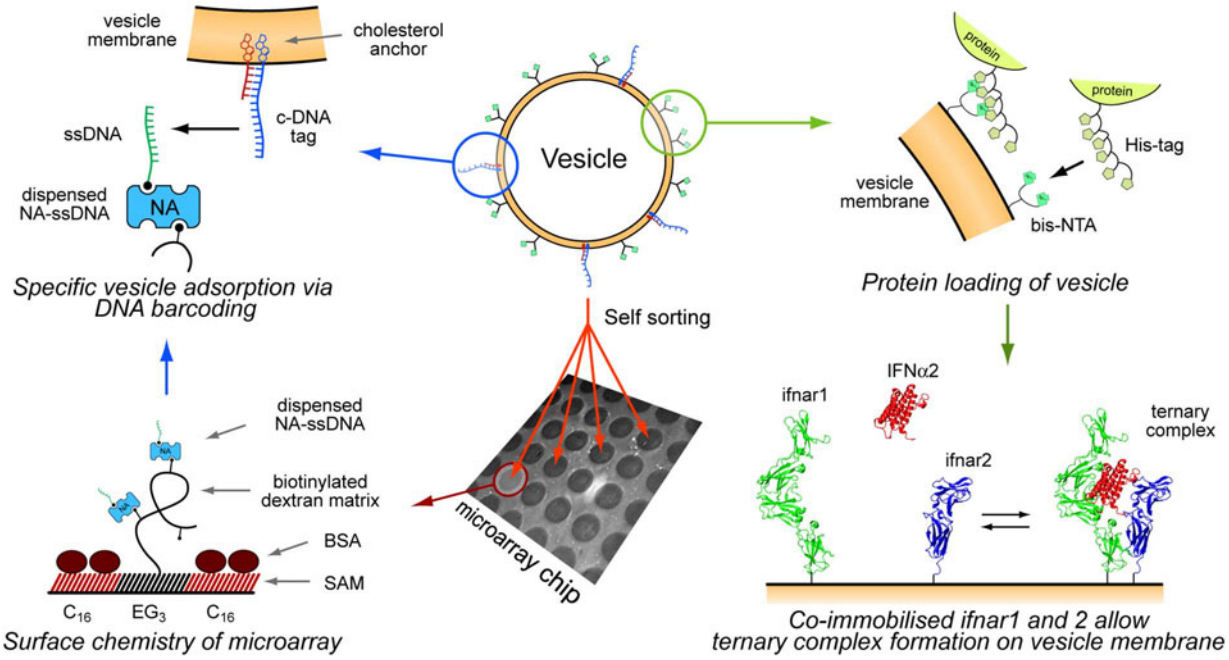

FIG. 1. Schematic of addressable adsorption of lipid vesicles via DNA bar coding onto a prestructured microarray chip, which is composed of dextran spots holding complementary DNA strands that are separated by hydrophobic domains modified with BSA. Also shown is protein loading of the vesicles via histidine tags and NTA chelators incorporated in the lipid membrane. Coimmobilization of the two receptor subunits ifnar1 and ifnar2 allow the study of ternary complex formation with the ligand IFNα2 through lateral diffusion of the receptor subunits in the membrane.

stranded DNA sequences (c-DNA) are introduced. Consequently, DNA hybridization leads to self-sorting and immobilization of the vesicles to their respective array sites. This approach was inspired by the work of Niemeyer *et al.*,[15,16] who used it to immobilize proteins to specific sites on a surface. The method offers stable tethering of the lipid vesicles to the surface while maintaining physiological conditions throughout the assay. c-DNA tagging of vesicles is readily performed by using cholesterol-modified oligonucleotides as the cholesterol end will spontaneously self-incorporate into the lipid bilayer of a vesicle.[12,13] To increase the stability of this integration, Pfeiffer and Höök[17,18] used two cholesterol-modified sequences, one long and one short, which are complementary to each other at the cholesterol end and hybridize with a resulting stronger, multivalent, bond to the membrane. The nonhybridized part of the longer strand is available for attachment to the surface ssDNA. We have used this approach in our work, schematically illustrated in Fig. 1, to immobilize DNA-tagged vesicles, which were subsequently functionalized with receptors for the study of their interaction with their ligand.

An underlying array was produced by microcontact printing (μCP),[19,20] which provides a hydrophobic grid of hexadecanethiol (C_{16})-SAM (self-assembled monolayer) on gold. The chip was then back-filled with alkanethiol that is terminated by triethylene glycol, which was subsequently modified with a biotinylated dextran hydrogel matrix.[21] Ink-jet printing[19,22] of ssDNA, which was modified with biotin and bound to neutravidin (NA), is then performed at specific sites of the surface. The hydrophobic C_{16} barriers aid in containing the dispensed solution in the spots, thereby hindering cross contamination of ssDNA. To passivate the hydrophobic regions, before mounting the chip in the instrument, they were covered by a layer of bovine serum albumin (BSA). The injected vesicles are bar coded with c-DNA and will self-sort on the surface upon specific interaction with the corresponding preimmobilized ssDNA-NA. The dextran layer provides a flexible support for the vesicles, and DNA hybridization is highly stable under normal conditions.

Additionally, the lipid membranes of the vesicles contain the bivalent chelator *bis*-nitrilotriacetic acid (*bis*-NTA), which is able to bind histidine-tagged proteins via coordination of chelated transition metal ions, e.g., Ni^{2+}.[23] Immobilization via NTA produces homogeneous, highly oriented, and functional protein layers,[24] and the binding is reversible with the addition of, e.g., imidazole. The *bis*-NTA has been shown to bind more firmly as compared to traditional monovalent NTA through multivalent interactions with the histidine tag,[25,26] which provide for more reliable protein interaction measurements. In this work, we chose to demonstrate protein loading and interaction analysis on the vesicles with the extracellular domains of the interferon I receptor, the subunits ifnar1 and ifnar2, which both contain a decahistidine tag (His_{10}) at the C terminus. Type I interferons elicit antiviral and antiproliferative responses in the body, which has made them important subjects of study in clinical research.[27] Ifnar1 and ifnar2, coimmobilized on a lipid membrane, were previously shown to form a ternary complex with their ligand IFNα2 via lateral diffusion on the membrane.[19,28–30] This feature is also confirmed in our study.

A visual demonstration of DNA-mediated sorting of functionalized vesicles was recently reported by Städler *et al.*[31]

DNA_X 5'-cholesterol-CCC-TCC-GTC-GTG-CCT-3'

DNA_A 3'-cholesterol-CCC-AGG-CAG-CAC-GGA-ACC-TGT-AGT-CTT-TAT-5'
5'-TGG-ACA-TCA-GAA-ATA-CCC-biotin-3' $DNA_{A'}$

DNA_B 3'-cholesterol-CCC-AGG-CAG-CAC-GGA-TTG-GAT-CAC-TCT-TTA-5'
5'-AAC-CTA-GTG-AGA-AAT-CCC-biotin-3' $DNA_{B'}$

DNA_C 3'-cholesterol-CCC-AGG-CAG-CAC-GGA-ATA-AAG-ACT-ACA-GGT-5'
5'-TAT-TTC-TGA-TGT-CCA-CCC-biotin-3' $DNA_{C'}$

DNA_D 3'-cholesterol-CCC-AGG-CAG-CAC-GGA-GTG-ATA-TAC-AAG-CAA-5'
5'-CAC-TAT-ATG-TTC-GTT-CCC-bitoin-3' $DNA_{D'}$

SCHEME 1. Modified DNA sequences used for bar coding. Complementarity is highlighted using color-coded sequences.

However, no real-time signal monitoring was presented and no subsequent biomolecular interaction was demonstrated with the functionalized vesicles. We, on the other hand, are hereby first (to our knowledge) to demonstrate the addressable adsorption of receptor-loaded vesicles on a microarray, where the whole assay, from vesicle adsorption to receptor-ligand interactions and regeneration, is monitored in real time. Even more important, the binding events were monitored label-free by using imaging surface plasmon resonance[32] (SPR) operating in ellipsometric mode.[19,33]

II. EXPERIMENTAL SECTION

In this work, four different DNA systems (designed by LayerLab AB, Sweden and purchased from MedProbe) were used, and are shown in Scheme 1 along with the terminal modifications of the strands and color-indicated complementarities between the strands. The left strands (A, B, C, D, and X) were incorporated into the vesicle membranes via the cholesterol end. DNA_X is complementary to 12 bases on each of the other four cholesterol strands and stabilizes the incorporation in the membrane as discussed above. The right strands (A′, B′, C′, and D′) are biotin modified and are immobilized in predefined array positions together with neutravidin.

A. Preparation of lipid vesicles

Chloroform-dissolved 1-palmitoyl-2-oleoyl-*sn*-glycero-3-phosphocholine (Avanti Polar Lipids) and octadec-9-enyl-octadecyl-amine-bis-nitrilotriacetic acid (*bis*-NTA; synthesis described in Ref. 30) were mixed 19:1, and the solvent was allowed to evaporate under a N_2 stream for 15 min and then under vacuum ($<10^{-6}$ mbar) for 1 h. The remaining powder was hydrated with HBS buffer (10 mM hepes, 150 mM NaCl, *p*H 7.4) to a concentration of 5 mg/mL and extruded 21 times through 100 nm pores in polycarbonate membranes (Whatman). The lipid vesicle solutions were divided and each mixed with a DNA solution consisting of two single strands: DNA_A+DNA_X, DNA_B+DNA_X, DNA_C+DNA_X, and DNA_D+DNA_X. Each pair was allowed to hybridize in a 1:1 molar ratio for at least 1 h before being mixed with its vesicle solution to a concentration of 0.1 μM. At least 1 h was thereafter given for a proper integration of the DNA-cholesterol into the vesicle membrane. Thus, four DNA-tagged vesicle solutions were produced, each with a unique DNA strand that has 15 bases that are available for hybridizing with complementary strands on the chip.

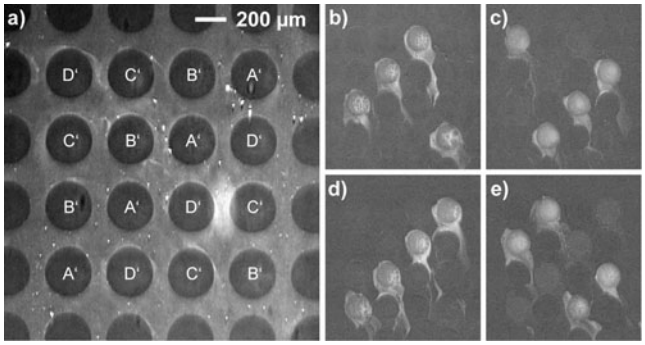

FIG. 2. Specific vesicle targeting. (a) The array seen with imaging SPR; intensity is proportional to adsorbed mass. Four different solutions of NA-ssDNA (A′, B′, C′, and D′) have been dispensed as indicated. [(b)–(e)] Difference images showing injection of vesicles tagged with DNA complementary to (b) B′, (c) D′, (d) A′, and (e) C′.

B. Preparation of microarray chips

SPR sensor substrates, gold on SF-10 glass, were manufactured and cleaned prior to use as described in our previous work.[19] The poly(dimethylsiloxane) stamp was produced as described elsewhere.[34] The pattern consists of 100-μm-wide protruding frames separating a 12×12 array of 300-μm-wide recessed circles. Prior to its use, the stamp was thoroughly rinsed in ethanol and dried in a stream of N_2. The stamp was inked for 60 s in 10 mM hexadecanethiol (C_{16}, Fluka) in ethanol and then dried in a stream of N_2. It was thereafter brought in contact with a clean gold substrate for 30 s, on which it generated 100-μm-wide hydrophobic SAM barriers of C_{16}. After printing, the surface was incubated in a solution of 0.5 mM tri(ethylene glycol) thiol [$HS\text{-}(CH_2)_{15}\text{-}CO\text{-}(OC_2H_4)_3\text{-}OH$, EG_3] (Ref. 35) in ethanol for 16 h. The surface was then modified with carboxylated dextran by using the protocol by Löfås and Johnsson.[21] However, instead of using 500 kDa dextran, we used 40 kDa (GE Healthcare). Before being dispensed, the surface was biotinylated by first activating the dextran matrix for 20 min in a mixture of 0.2*M* *N*-ethyl-*N*′-(3-dimethylaminopropyl) carbodiimide hydrochloride and 0.05*M* *N*-hydroxysuccinimide in water. Then, the surface was incubated in 5 mM biotin-amine (Molecular Biosciences) for 20 min in MilliQ water and, finally, unreacted esters were deactivated for 20 min with 1*M* ethanolamine, also in MilliQ.

The solutions to be dispensed consisted of NA (0.8 μM, Invitrogen) together with four different biotin-modified ss-DNA strands (1.6 μM, MedProbe), as shown in Scheme 1 (A′, B′, C′, and D′). Each NA-ssDNA solution was dispensed in four spots, yielding the 4×4 array, which can be seen in Fig. 2(a). The solutions were dispensed with a 60-μm-diameter piezoelectrically driven glass capillary (Microdrop) with a manual x/y stage for positioning the surface. The humidity in the room was above 80% and the surface was cooled (slightly) below the dew temperature for two reasons: (1) to hinder the evaporation of dispensed droplets and (2) to reveal the μCP pattern due to contrast in con-

densed water formation on C_{16} and EG_3-dextran regions, which was required for positioning the ink-jet head. Two droplets were dispensed on each spot, giving a volume of roughly 0.5 nL (assuming a dispensed droplet diameter of 60 μm). The dispenser was thoroughly cleaned between solutions by sonicating the tip at 12 kHz in MilliQ water, 50 mM NaOH, and then ethanol. Having dispensed the last solution, after 15 min, the chip was thoroughly rinsed in MilliQ water and then incubated in 1 mg/mL BSA (Sigma) in HBS for 15 min. Prior to docking in the instrument, the surface was thoroughly rinsed in MilliQ water and dried in a stream of N_2.

C. Imaging SPR

The instrument used was an imaging null ellipsometer (EP3, Nanofilm, Germany) equipped with a SPR cell based on the Kretschmann setup[36] with a 60° SF-10 prism and connected to a ~10 μL flow cell. A xenon lamp was used as a light source, and the wavelength was selected by an interference filter. The combination of imaging ellipsometry and SPR was used before to monitor biomolecular interactions in different regions of a surface in parallel.[19,37] The instrument was used in two modes, of which the first is the intensity mode where only the intensity of reflected *p*-polarized light is recorded by the charge coupled device detector. This mode is characteristic of traditional imaging SPR (also known as SPR microscopy).[38] The change in intensity of the reflected light is directly proportional to the material adsorbed on the gold surface, which makes interpretation of data simple. The other mode of operation is ellipsometric, where the phase changes in the reflected light are monitored and represented by the ellipsometric angle Δ, which has been averaged for each region of interest. For the parameter set used in our experiments, Δ is inversely proportional to the adsorbed mass to the gold chip. The instrument was mainly used in the ellipsometric Δ mode and was switched to the intensity mode for recording images of the surface at the indicated times in the text. Four images were recorded in sequence and averaged into one, at each event, to reduce noise. Difference images were produced by subtracting the image after a certain event with the image before. The angle of incidence was 62°, and the wavelength was 532 nm for the intensity mode and 559 nm for the ellipsometric mode.

D. Binding assays

After mounting the chip, it was conditioned with an injection of MilliQ water (7 min), 50 mM NAOH (2×1 min), and 1 mg/mL BSA in HBS (7 min). The lipid vesicle solutions were diluted ten times and injected together with 1 mM imidazole. Subsequently, the NTA moieties were loaded by an injection of 100 μM $NiCl_2$. The extracellular domains of type I interferon receptor subunits ifnar1 and ifnar2 fused to a C-terminal decahistidine tag (ifnar1-His_{10} and ifnar2-His_{10}, respectively) were tethered onto the adsorbed vesicles and their interaction with the ligand IFNα2 was monitored. Wild type (wt) Ifnar1-His_{10} was used as well as wt ifnar2-His_{10} and two mutants (E79A and W109A) with reduced affinity toward the ligand IFNα2. For ligand binding assays, IFNα2 and a mutant with 100-fold reduced affinity toward ifnar2 (M148A) were employed.[39] Expression, purification, and characterization of the interaction of these proteins and the mutants were described previously.[29,39–41] All measurements were performed in HBS buffer. A continuous flow injection system was used, running constantly at 10 μL/min, except during ligand injection, in which the flow rate was doubled in order to minimize mass transport effects. No quantitative kinetic analyses of the receptor-ligand interaction curves were performed because the flow cell of the system was not optimized, which yields a relatively high diffusion layer thickness. Instead, we have limited the analyses to a qualitative nature.

III. RESULTS AND DISCUSSION

The basic principle for the addressable immobilization of lipid vesicles and their subsequent protein loading with histidine-tagged proteins are illustrated in Fig. 1. A microarray is produced, consisting of circular regions (300 μm diameter) of a dextran hydrogel that have been modified with distinct sequences of ssDNA via neutravidin-biotin chemistry. The circular regions are separated by a hydrophobic barrier SAM, which has been covered by BSA. Lipid vesicles are prepared with c-DNA sequences and will hybridize with their matching counterparts on the surface, i.e., self-sort on the array (see Scheme 1). Incorporation of the DNA into the lipid membrane is achieved by having (bivalent) cholesterol-modified DNA strands. The dispensed ssDNAs are named A′–D′ and their corresponding c-DNAs on the vesicles are termed A–D. The vesicles also contain the multivalent chelator *bis*-NTA, which enables stable and highly oriented immobilization of histidine-tagged proteins to its membrane.

A. Addressable vesicle adsorption

Figure 2(a) shows a SPR image of the chip after it has been docked in the instrument together with the positions of dispensed $ssDNA_{A'-D'}$. Figures 2(b)–2(e) are SPR difference images showing the addressable vesicle adsorption to the chip; vesicles tagged with c-DNA_B [Fig. 2(b)], c-DNA_D [Fig. 2(c)], c-DNA_A [Fig. 2(d)], and c-DNA_C [Fig. 2(e)] were injected in sequence. Apparent in all images is a "comet tail" associated with each spot, which has been observed elsewhere as well.[42] This is an effect of the rinsing of the dispensed chip during manufacturing, which has resulted in physisorption of surplus NA-ssDNA on the hydrophobic C_{16} framework. It can be seen that this brief physisorption process was very efficient, as the resulting vesicle adsorption produced equally or, in some cases, even better signals than the dextran-immobilized NA-ssDNA. This high signal is mainly believed to stem from the closer proximity to the surface and, thus, from a more intense surface plasmon field. Although this presents an alternative, simpler, immobilization strategy for the NA-ssDNA, it does not offer an equally stable immobilization, as physisorbed proteins can be replaced by other proteins or by low-molecule com-

pounds.[43–45] A stable vesicle immobilization is vital for reliable, subsequent protein interaction measurements. It can also be seen that although the comet tail has reached a dextran spot, no cross contamination has occurred (or, alternatively, is to low too be detected) in that spot, most likely because of a slower immobilization rate to dextran (data not shown). The comet-tail appearance of the microarrays is therefore a minor, mainly aesthetic, problem that can be solved by optimizing the production protocols.

A high degree of specific vesicle binding to the spots of the correct corresponding sequence on the array was noted from the images. Unspecific binding to the BSA-covered framework or nondispensed dextran spots is nonexistent or below the detection limits of the instrument. In Fig. 2(d), a small binding of c-DNA_C-tagged vesicles was observed on ss$DNA_{A'}$ dispensed regions, due to full sequence complementarity between c-DNA_C and c-DNA_A (see Scheme 1), which leads to specific vesicle association, that is, vesicle multilayer formation.[46,47] However, the signal is very low as the second vesicle layer is located further away from the surface and is therefore expected to produce a much weaker SPR signal in subsequent interaction studies. Note that the evanescent probe depth is ~ 50 nm under the optical parameters used,[36] which is significantly shorter than when vesicle multilayers were used as a means to increase the signal in SPR analysis.[46]

B. Online protein loading and cross contamination of vesicles

In order to probe selective protein targeting to different array elements, the binding of IFNα2 to wild-type ifnar2-His_{10} as well as the mutants W102A and E79A was monitored. IFNα2 binds wild-type ifnar2-His_{10} with an equilibrium dissociation constant of ~ 5 nM and dissociates with a rate constant of ~ 0.01 s^{-1}. The binding affinity toward the mutants W102A and E79A is reduced, which leads to three and ten times faster dissociation kinetics, respectively.[41] Thus, the ifnar2 mutants can be discriminated by the ligand dissociation kinetics. The online protein loading of the vesicles via histidine tags proved to be problematic. Figure 3(a) shows sensorgrams from the four different dispensed regions of the microarray during an experiment where vesicles were injected in sequence, each followed by a 100 μM Ni^{2+} injection, followed by protein loading. The first three vesicles were loaded with receptors and the last was only loaded with Ni^{2+} to act as a negative control for the ligand injection. The steps in the experiment, as indicated in Fig. 3, are (1) c-DNA_C vesicle, (2) 1 μM ifnar2-His_{10} E79A, (3) c-DNA_D vesicle, (4) 1 μM ifnar2-His_{10} W102A, (5) c-DNA_A vesicle, (6) 1 μM ifnar2-His_{10} wt, (7) c-DNA_B vesicle, (8) 1 μM ligand IFNα2, and (9) 1*M* imidazole. It is important to note that the order of receptor loading was chosen to follow the affinity of the proteins to their ligand, that is, E79A has the fastest dissociation rate, followed by W102A, and then wt.

A comparison of the sensorgrams obtained on array elements shows that the adsorption of vesicles is highly specific. There is neither unspecific adsorption to other dispensed spots nor to undispensed dextran or BSA reference areas. We have noted, however, that unspecific binding of vesicles to dispensed areas with already adsorbed vesicles with loaded proteins does occur if the vesicles are injected without a low concentration of imidazole. This is a likely interaction effect between the *bis*-NTA on the injected vesicles and the histidine tag of loaded proteins on previously adsorbed vesicles. The histidine tags used are ten units long, and there is a potential risk that portions of them are free, as each *bis*-NTA is theoretically capable of binding to four histidines. Thus, by adding 1 mM imidazole to the vesicle solutions to be injected, their *bis*-NTA chelators are effectively shielded from interaction with histidine tags. This concentration gives a $\sim 30\times$ surplus of imidazole to available NTA, but is too low to cause a dissociation of vesicle-loaded proteins.[35] Some unspecific histidine-tagged receptor adsorption to the surface was observed, though, but it seemed not to influence the experiments.[48]

Injection of the ligand (event 8) leads to specific responses on signals where receptors have been loaded, and no response is seen on the negative control (B′ signals). It is also evident that 1*M* imidazole is an effective strategy to remove the histidine-tagged proteins without disturbing the vesicle structure noticeably, as the levels return to their initial proteinless values. When the vesicles were reloaded with protein, the signals reached the same levels as in the first loading (data not shown).

In order to analyze potential cross contamination by this sequential protein loading procedure, the binding kinetics obtained on different array elements was explored. Figure 3(b) shows the normalized dissociation of the ligand from the loaded proteins of the microarray (after event 8). In Fig. 3(c), the dissociation curves obtained in this multiplexed experiment were overlaid with the reference dissociation curves for ifnar2-His_{10} wt, E79A, and W102A, which were obtained in separate binding experiments (data not shown). The only dissociation curve overlapping with its reference curve is the A′ system, which was last loaded with proteins (wt) and is the only one that has not been mixed with other proteins. The C′ and D′ systems, however, have shifted their dissociations to slower rates, i.e., they have both been blended with subsequent protein loadings. The C′ system, which was intended to be loaded with E79A, has been blended with both W102A and wt, and the D′ system, originally loaded with W102A, has attracted the wt. Thus, our findings suggest that in the case where pure protein populations on each vesicle are desired, it is vital that the vesicles are loaded offline prior to injection. Offline loading would, however, require larger amounts of proteins to obtain reasonable immobilization levels. On the other hand, the potential drawback of employing online loading of proteins can also be turned into a very powerful advantage for studies of multiprotein binding phenomena on the vesicle surface—a set of experiments that we describe below.

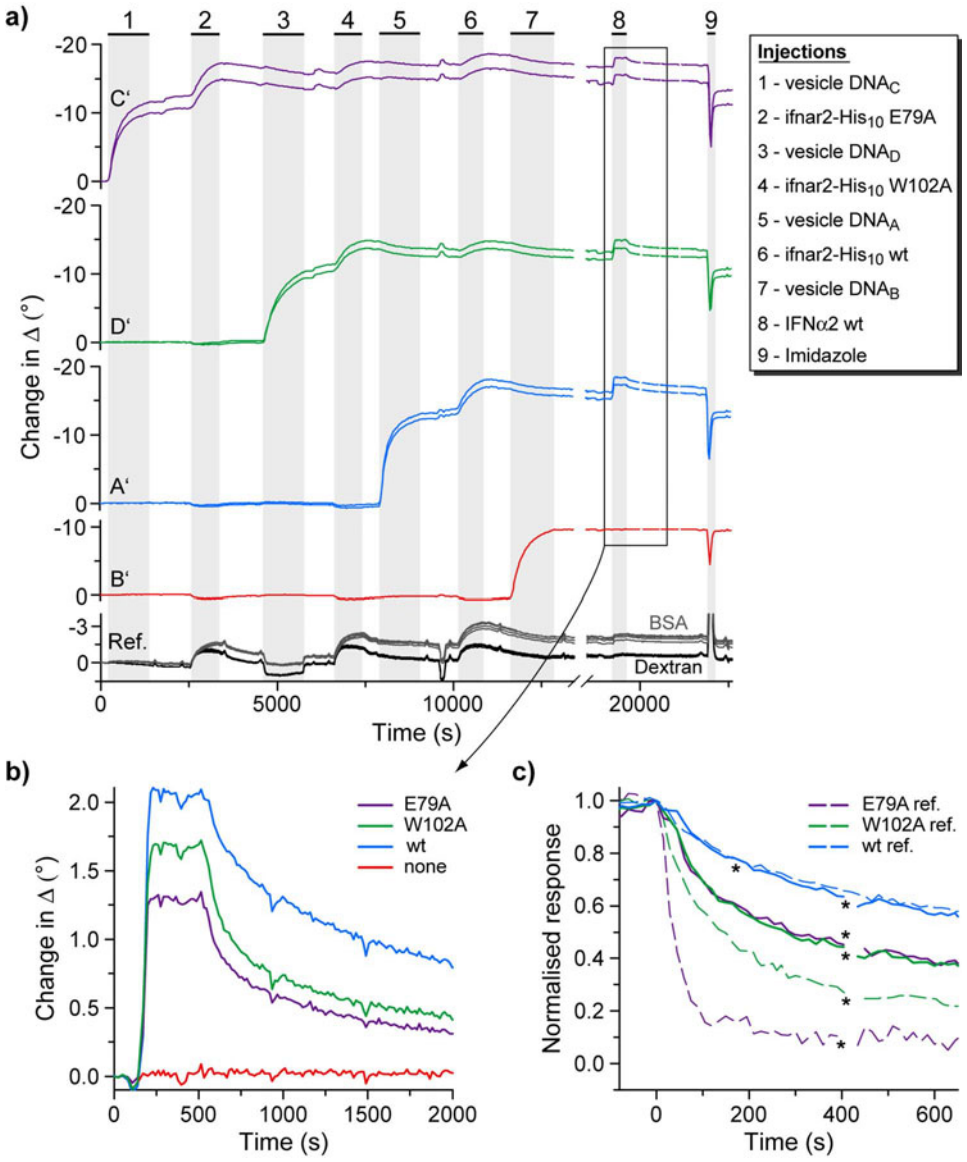

FIG. 3. Addressable adsorption of lipid vesicles followed by online protein loading, resulting in cross contamination. (a) Color-coded reference (dextran) subtracted signals from the 4×4 spots of the chips. Injection events are indicated in the table. After the injection of differently DNA bar-coded vesicles (1, 3, 5, and 7), they are loaded with different variants of ifnar2-His$_{10}$: ifnar2-His$_{10}$ E79A (2), ifnar2-His$_{10}$ W102A (4), and ifnar2-His$_{10}$ wt (6). Injection of 1*M* imidazole was efficient in removing the proteins (9). Four unmodified reference signals (note that the *y* scale is expanded) are also shown from BSA and dextran regions, respectively. Only 7 signals out of 16 are shown as an accidental air injection unfortunately covered and destroyed 9 spots of the array during the course of the experiment. (b) Close-up of the ligand interaction (8) with the vesicles (averaged signals) color coded as in (a) and according to the intended receptor loading. Unloaded vesicles (B′) show no ligand interaction (negative control). (c) Normalized (and averaged) ligand dissociation curves. The dashed lines are reference curves, previously measured, of vesicles loaded with only one receptor. The color coding corresponds to the intended loading of the vesicles in (a). It is apparent that the dissociation curves of signals C′ and D′ have been shifted to slower dissociation as compared to their respective reference curves, E79A and W102A, indicating cross binding from subsequent protein injections. The only dissociation curve coinciding with its reference curve is the A′ signal, which is consistent with the fact that it was the last injected receptor (wt). Disturbing pressure pulses from the pump have been omitted in the curves at position indicated by *.

C. Study of a ternary complex formation

The living cell is a dynamic system of many biomolecules interacting with each other. Often the interactions are complex and involve more than two species. In particular, for transmembrane signaling, ligand-induced assembly of multiprotein complexes plays an important role. It is therefore of great interest to be able to study mixed multicomponent surfaces/assays. We decided to demonstrate this with our microarray platform by using the online cross-binding effect to produce mixed populations of two receptor subunits on each vesicle membrane with the intention of differentiating between binary (receptor-ligand) and ternary (receptor-ligand-receptor) complex formations with their ligand. Hence, a truly multiplexed assay was attempted. For these assays, IFNα2 M148A was employed, which binds ifnar2-His$_{10}$ with ~100-fold faster dissociation rate constant compared to wild-type IFNα2, but with unchanged binding affinity toward ifnar1-His$_{10}$.[41] Thus, binary and ternary complexes can

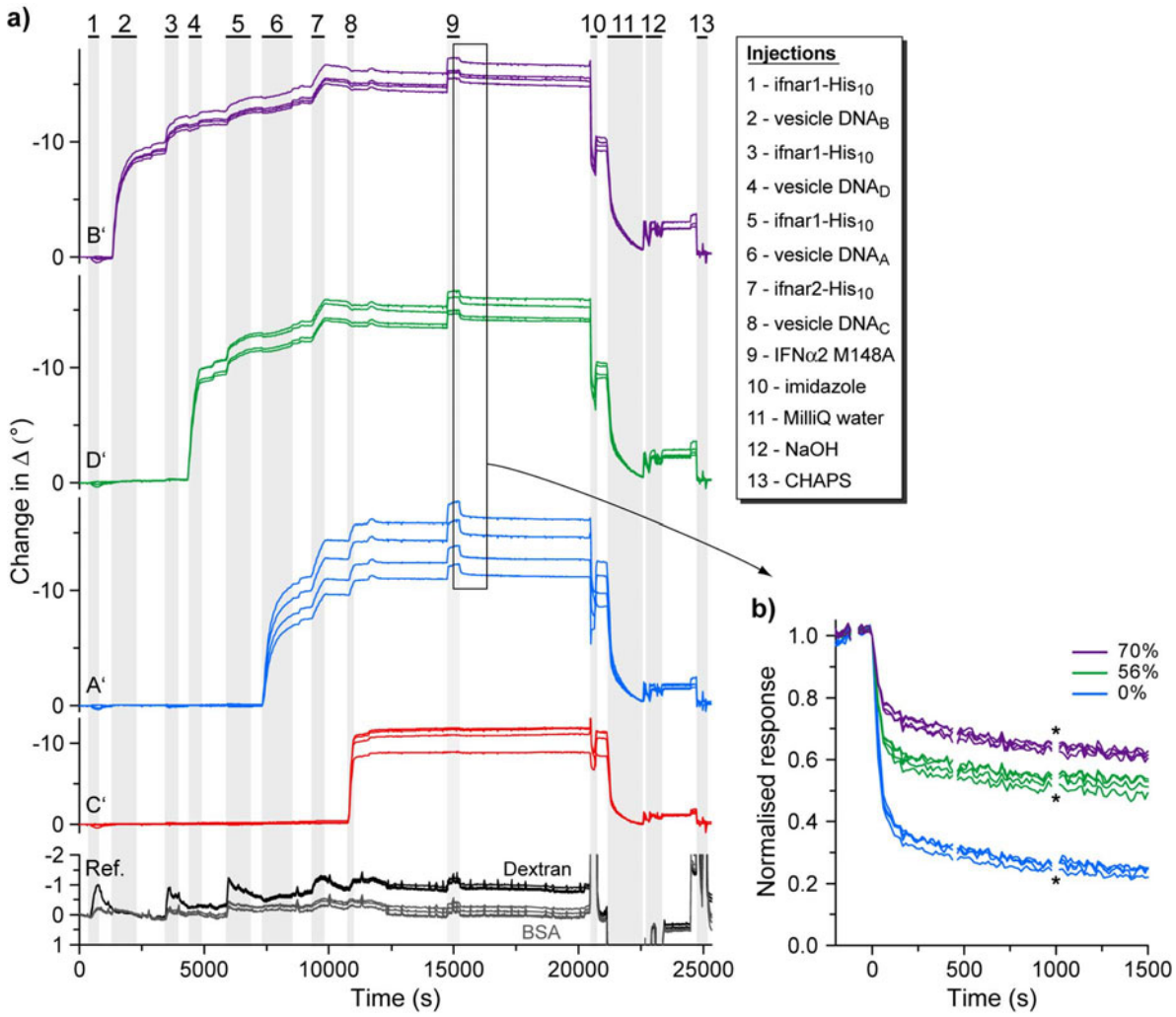

FIG. 4. Formation of a ternary complex between the receptor subunits ifnar1 and ifnar2 and the ligand IFNα2 M148A. (a) Reference (dextran) subtracted sensorgrams from the 4×4 signals of the microarray together with four unmodified reference curves (note their expanded y scale) from both dextran and BSA regions. Injection events are indicated in the table. The last injected vesicle (8) was not loaded with receptor and acts as a negative control for the ligand injection (9). (b) Normalized dissociation curves of the 12 spots with receptors after interaction with the ligand (9). The curves differentiate themselves in groups of four, according to the dispensed ssDNA strands, with a high degree of overlap. The fractions of ifnar1 relative to the total amount of receptor subunits loaded on vesicles are indicated. Disturbing pressure pulses from the pump have been omitted in the curves (noted by *).

be more efficiently discriminated in the case of the fast dissociating mutant M148A compared to wild-type IFNα2.

In general, the experiment in Sec. III B was repeated, with the major difference that the loaded proteins were only two: the receptor subunits ifnar1-His_{10} and ifnar2-His_{10} (both wt), coimmobilized in different compositions on the vesicles. Figure 4(a) shows this experiment and the indicated events are (1) 300 nM ifnar1-His_{10} (control injection), (2) c-DNA_B vesicle, (3) 300 nM ifnar1-His_{10}, (4) c-DNA_D vesicle, (5) 300 nM ifnar1-His_{10}, (6) c-DNA_A vesicle, (7) 500 nM ifnar2-His_{10}, (8) c-DNA_C vesicle, (9) 1 μM IFNα2 M148A, (10) 1*M* imidazole, (11) MilliQ water, (12) 50 mM NaOH, and (13) 20 mM 3-[(3-cholamidopropyl)dimethylammonio]-1-propanesulfonate (CHAPS, Fluka). The sensorgrams show consistent results with the previous experiment. All the signals were successfully monitored during the whole experiment, and the signals of each system show a good degree of repeatability.[49]

The negative control, once again, did not respond to the injection of ligand, and the injection of imidazole was efficient in removing loaded histidine-tagged proteins from the vesicles. An injection of MilliQ water is efficient in removing the c-DNA-tagged vesicles, due to dehybridization of the double-stranded DNA by removing stabilizing cations,[50] but not completely. Instead, an injection of the detergent CHAPS is able to bring the signals back to the original baseline. However, we have found that the microarray is not completely regenerated by this treatment (MilliQ+CHAPS), nor by NaOH solutions (up to 50 mM; data not shown), as subsequent DNA-loaded vesicle injections fail to adsorb up to the same signal levels as in the first cycle. Most likely, alternative ways, e.g., raised temperatures (which we were not able to test in our flow system), might be needed to break the hybridized DNA and to free the surface sites for rebinding and, thus, reuse of the chip.

From the SPR curves, calculated fractions of ifnar1 to total amount of receptor subunits loaded on vesicles are $70 \pm 1\%$ for the B′ system, $56 \pm 1\%$ for the D′ system, and 0 for the A′ system. The normalized dissociation of IFNα2 M148A from the receptor populations of these vesicles is shown in Fig. 4(b). As the lipid membrane allows lateral diffusion of the immobilized receptors, coimmobilization of ifnar1 and infar2 can result in the formation of a ternary complex with their ligand (Fig. 1), which was previously shown.[19,28–30] The mutant ligand was chosen as it has a lower affinity to ifnar2 as compared to the wt and would make differences in dissociation possible to distinguish with the data sampling rate of our instrument. In Fig. 4(b), it can be seen that as the ratio of ifnar1 of the vesicles increases, the dissociation of the ligand decreases. The ligand affinity of ifnar1 alone is at least one order of magnitude lower than that of ifnar2 toward IFNα2 M148A,[28,29] and the observed effect is ascribed to a ternary complex formation on the fluid lipid membrane as the receptor subunits simultaneously interact with the ligand, as illustrated in Fig. 1. Our results are consistent with previous studies on solid-supported membranes where much slower dissociation of the ternary complex was observed compared to the binary (roughly a factor of 100).[29] The dissociation curves are also consistent with the receptor mixtures, and the high degree of overlap within the replicas indicates good repeatability and quality of the assay.

IV. CONCLUSIONS

We have demonstrated the microfabrication of a microarray for the addressable adsorption of c-DNA-tagged lipid vesicles. Furthermore, monitoring interactions of biomolecules loaded on the vesicles has been shown with an interferon I receptor-ligand model system. The microarray consisted of four different DNA barcodes, each dispensed in four replicates. The specificity of vesicle targeting was shown to be very high, as no unspecific DNA adsorption was detected. Due to a limited amount of material, the vesicles were loaded online with protein (adsorbed to the chip). This was shown to produce cross binding between vesicles, which means that in cases wherein pure protein populations on the vesicles are desired, vesicle loading should therefore be performed offline prior to vesicle immobilization. This potential weakness was turned into an advantage by coimmobilizing two receptor subunits in different ratios on spatially separated vesicles on the array format, which were further utilized to investigate their ternary complex formation with the ligand. Thus, this approach allows for complex studies of multicomponent systems in a controlled manner.

A benefit of our approach is that it allows a virtually limitless capacity in terms of the amount of systems that can be put on a surface, due to the high combinatorial variability and specificity of DNA, which would truly allow parallelized, high-throughput analyses. In addition, the microarray can also be used for the addressable adsorption of other type of species with c-DNA tags, e.g., antibodies,[15,16] and membrane-residing proteins, which offers a stable, mild, and efficient immobilization procedure.

ACKNOWLEDGMENTS

This research was supported by grants from the Wallenberg Consortium North (WCN) and the Swedish Foundation for Strategic Research (SSF) through the Biomimetic Materials Science program. J.P. acknowledges funding from the DFG (Grant Nos. PI-405/1 and PI 405/2). T.E. achnowledges the Carl Tryggers Foundation for financial support.

[1]C. Harrington, C. Rosenow, and J. Retief, Curr. Opin. Chem. Biol. **3**, 285 (2000).
[2]M. J. Heller, Annu. Rev. Biomed. Eng. **4**, 129 (2002).
[3]C. Niemeyer and D. Blohm, Angew. Chem., Int. Ed. **38**, 2865 (1999).
[4]M. Templin, D. Stoll, M. Schrenk, P. Traub, C. Vohringer, and T. Joos, Trends Biotechnol. **20**, 160 (2002).
[5]M. Templin, D. Stoll, J. Schwenk, O. Potz, S. Kramer, and T. Joos, Proteomics **3**, 2155 (2003).
[6]H. Zhu and M. Snyder, Curr. Opin. Chem. Biol. **5**, 40 (2001).
[7]B. Alberts, D. Bray, J. Lewis, M. Raff, K. Roberts, and J. D. Watson, *Molecular Biology of the Cell*, 3rd ed. (Garland, New York, 1994).
[8]J. Drews, Science **287**, 1960 (2000).
[9]E. Sackmann, Science **271**, 43 (1996).
[10]C. Bieri, O. Ernst, S. Heyse, K. Hofmann, and H. Vogel, Nat. Biotechnol. **17**, 1105 (1999).
[11]Y. Fang, A. Frutos, and J. Lahiri, J. Am. Chem. Soc. **124**, 2394 (2002).
[12]B. Stadler, D. Falconnet, I. Pfeiffer, F. Hook, and J. Voros, Langmuir **20**, 11348 (2004).
[13]S. Svedhem, I. Pfeiffer, C. Larsson, C. Wingren, C. Borrebaeck, and F. Höök, ChemBioChem **4**, 339 (2003).
[14]C. Yoshina-Ishii and S. Boxer, J. Am. Chem. Soc. **125**, 3696 (2003).
[15]C. Niemeyer, L. Boldt, B. Ceyhan, and D. Blohm, Anal. Biochem. **268**, 54 (1999).
[16]C. M. Niemeyer, T. Sano, C. L. Smith, and C. R. Cantor, Nucleic Acids Res. **22**, 5530 (1994).
[17]I. Pfeiffer and F. Höök, J. Am. Chem. Soc. **126**, 10224 (2004).
[18]I. Pfeiffer and F. Höök, Anal. Chem. **78**, 7493 (2006).
[19]G. Klenkar, R. Valiokas, I. Lundstrom, A. Tinazli, R. Tampe, J. Piehler, and B. Liedberg, Anal. Chem. **78**, 3643 (2006).
[20]Y. Xia and G. Whitesides, Angew. Chem., Int. Ed. **37**, 550 (1998).
[21]S. Löfås and B. Johnsson, J. Chem. Soc., Chem. Commun. **1990**, 1526.
[22]A. Roda, M. Guardigli, C. Russo, P. Pasini, and M. Baraldini, BioTechniques **28**, 492 (2000).
[23]K. Busch and R. Tampé, Rev. Mol. Biotechnol. **82**, 3 (2001).
[24]G. B. Sigal, C. Bamdad, A. Barberis, J. Strominger, and G. M. Whitesides, Anal. Chem. **68**, 490 (1996).
[25]S. Lata and J. Piehler, Anal. Chem. **77**, 1096 (2005).
[26]S. Lata, A. Reichel, R. Brock, R. Tampe, and J. Piehler, J. Am. Chem. Soc. **127**, 10205 (2005).
[27]R. Deonarain, D. C. Chan, L. C. Platanias, and E. N. Fish, Curr. Pharm. Des. **8**, 2131 (2002).
[28]M. Gavutis, S. Lata, P. Lamken, P. Muller, and J. Piehler, Biophys. J. **88**, 4289 (2005).
[29]P. Lamken, S. Lata, M. Gavutis, and J. Piehler, J. Mol. Biol. **341**, 303 (2004).
[30]S. Lata, M. Gavutis, and J. Piehler, J. Am. Chem. Soc. **128**, 6 (2006).
[31]B. Stadler, M. Bally, D. Grieshaber, J. Voros, A. Brisson, and H. M. Grandin, BioInterphases **1**, 142 (2006).
[32]J. M. Brockman, B. P. Nelson, and R. M. Corn, Annu. Rev. Phys. Chem. **51**, 41 (2000).
[33]F. Abelès, Surf. Sci. **56**, 237 (1976).
[34]Y. Zhou, R. Valiokas, and B. Liedberg, Langmuir **20**, 6206 (2004).
[35]A. Tinazli, J. Tang, R. Valiokas, S. Picuric, S. Lata, J. Piehler, B. Liedberg, and R. Tampe, Chem.-Eur. J. **11**, 5249 (2005).
[36]H. Raether, *Surface Plasmons on Smooth and Rough Surfaces and on Gratings* (Springer-Verlag, Berlin, 1988).
[37]R. Valiokas, G. Klenkar, A. Tinazli, R. Tampe, B. Liedberg, and J. Pie-

hler, ChemBioChem **7**, 1325 (2006).
[38]B. Rothenhausler and W. Knoll, Nature (London) **332**, 615 (1988).
[39]J. Piehler, L. Roisman, and G. Schreiber, J. Biol. Chem. **275**, 40425 (2000).
[40]J. Piehler and G. Schreiber, J. Mol. Biol. **289**, 57 (1999).
[41]J. Piehler and G. Schreiber, J. Mol. Biol. **294**, 223 (1999).
[42]L. Mezzasoma, T. Bacarese-Hamilton, M. Di Cristina, R. Rossi, F. Bistoni, and A. Crisanti, Clin. Chem. **48**, 121 (2002).
[43]J. Bohnert and T. Horbett, J. Colloid Interface Sci. **111**, 363 (1986).
[44]M. Mrksich and G. Whitesides, Annu. Rev. Biophys. Bioeng. **25**, 55 (1996).
[45]M. Wahlgren and T. Arnebrant, Trends Biotechnol. **9**, 201 (1991).
[46]A. Granéli, J. J. Benkoski, and F. Höök, Anal. Biochem. **367**, 87 (2007).
[47]A. Granéli, M. Edvardsson, and F. Höök, ChemPhysChem **5**, 729 (2004).
[48]The reference patches (BSA and dextran) show nonspecific adsorption of histidine-tagged receptors. This adsorption seems to be of a highly unstable nature as it bleeds completely off the surface with time. A related observation from the experiment is that when the vesicles were loaded with a relatively high concentration of receptor proteins, a certain loading level was passed, after which an unstable immobilization can be seen (dissociation). However, the dissociation levels off at a value at which it is stable. When lower amounts of proteins were injected, below that value, the immobilization was observed to be stable from the start (data not shown). We believe this to be the result of an interaction between the histidine-tagged and loosely associated ions (Ni^{2+}) on the surface (i.e., the BSA, dextran, and c-DNA tags of the vesicles).
[49]The B′ and D′ systems show a higher degree of repeatability in the signals compared to the A′ and C′ systems, which display a higher internal variance. This variation is an effect of the dispensing protocol; as the dispensing was manual and the location of the dispensing spots had to be revealed, water was evaporated on the array. Ideally, dispensing should occur as soon as the pattern is visible, but, in many cases, it got delayed and the formation of larger condensation droplets of water occurred before the spot was covered with the dispensing NA-ssDNA solution. Diffusion of proteins into the water droplets is relatively slow, which means that these areas of the spots will only partially be modified by NA-ssDNA and cannot fully interact with the vesicles. However, the variation remains consistent (proportional) throughout the whole time and is easily resolved by scaling as is shown ahead.
[50]G. L. Zubay, *Biochemistry*, 4th ed. (Brown, Dubuque, IA, 1998).